Stress Concentration Ratio and Design Method for Stone Columns using 2D FEA with Equivalent Strips

Ratio de concentration de contraintes et méthode de conception pour les colonnes ballastées en utilisant une analyse aux éléments finis 2D avec des bandes équivalentes

Poon B., Chan K.
GHD Geotechnics, 57-63, Herbert Street, Artarmon, NSW, Australia

ABSTRACT: This paper presents an approach for the prediction of vertical and horizontal displacements of soft ground treated with stone columns in a 2D finite element analysis (FEA). This involved modeling the columns as strips with appropriate strip width, spacing and smeared properties based on stress concentration ratio. Charts to assess the equivalent 2D column stress concentration ratio are provided for the design of full depth and floating columns under the influences of various key parameters. The accuracy of the proposed 2D strip model is investigated by comparing the results with a baseline 3D and axi-symmetric FEA. It is found that the proposed strip model is preferable over the conventional approach using composite block properties to represent the improved soil.

RÉSUMÉ : Cet article représente une approche pour la prédiction des déplacements verticaux et horizontaux de sols mous traités avec des colonnes ballastées par une analyse aux éléments finis (FEA) en 2D. Cela implique la modélisation des colonnes en tant que bandes avec une largeur de bande appropriée ainsi que l'espacement et les propriétés des zones d'influence basées sur le ratio de concentration de contrainte. Les graphiques pour évaluer le ratio 2D équivalent de concentration de contraintes sont donnés pour la conception des colonnes profondes et flottantes sous l'influence de divers paramètres. La précision du modèle de bande 2D proposé est étudiée en comparant les résultats avec une base en 3D et d'une analyse aux éléments finis axisymétrique. Il se trouve que le modèle de bande proposé est préférable à l'approche conventionnelle qui utilise les propriétés d'un bloc composite pour représenter le sol amélioré.

ORDS: Stone column, stress concentration, ground improvement, numerical analysis.

1 INTRODUCTION

Conventionally, the design of stone columns involves the prediction of settlements using a composite material approach in which equivalent strength and deformation parameters are derived using semi-empirical correlation to represent the entire improved soil. While these approaches have been accepted as reasonable methods for settlement prediction, they are less certain for the prediction of horizontal displacement. This paper presents a design approach where stone columns are idealised as equivalent strips in 2D finite element analysis (FEA). The stress distribution between the stone column and surrounding soil is essential for determining the strength parameter of the equivalent strips. A series of design curves for the stress concentration are presented to facilitate parameter derivation in practice. The accuracy of the 2D strip model is investigated by comparing the results with the 3D and axi-symmetric FEA.

2 IDEALISED 2D MODELLING APPROACH

For the modeling of stone columns in 2D FEA, the width of the stone column strips can be made to be equal to the width of an equivalent square for the cross-sectional area (Figure 1). The spacing of the strips is equal to the actual spacing, b, for square column arrangement and $\sqrt{3}b/2$ for equilateral triangular arrangement. Mohr-Coulomb model is used for the stone columns with Poisson's ratio of 0.3, which is taken to be the same as the soil itself. The equivalent Young's modulus E_{eq} and the cohesion c_{eq} of the strips can be calculated based on weighted average approach as given by Eq 1.

$$E_{eq}(or\ c_{eq}) = \frac{E_{soil}(or\ c_{soil})\cdot A_{soil} + E_{column}(or\ c_{column})\cdot A_{column}}{A_{soil}+A_{column}} \quad (1)$$

where A_{soil} and A_{column} are the areas of the soil and column inside a unit cell within the 2D strip as shown in Figure 1.

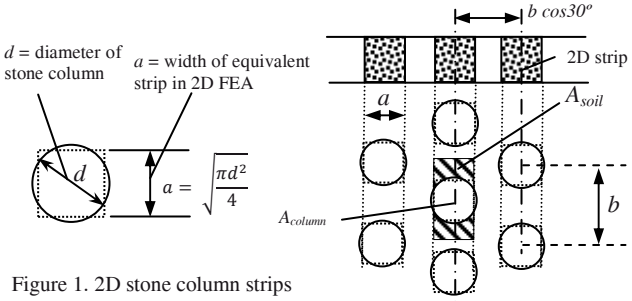

Figure 1. 2D stone column strips

The equivalent friction angle ϕ_{eq} of the strips can be derived based on force equilibrium approach as given by

$$tan(\phi_{eq}) = \frac{A_{soil}\tan(\phi_{soil}) + n\cdot A_{column}\tan(\phi_{column})}{A_{soil}+n\cdot A_{column}} \quad (2)$$

The determination of ϕ_{eq} requires a presumption of stress concentration, n, which is defined as the ratio of the average applied vertical stress within stone column to the average applied vertical stress of the surrounding soil at the same level. Section 3 presents an appraisal for this parameter. Note that the present 2D FEA is an elasto-plastic analysis in which the decay of excess pore pressure with time was not taken into account.

3 STRESS CONCENTRATION OF STONE COLUMN

This section presents a series of elasto-plastic solutions in charts for the stress concentration (n) of stone columns founded on (i) rigid boundary and (ii) infinite compressible soil materials. The solutions were obtained based on axisymmetric FEA using PLAXIS software programme for a "unit cell" consisting of a stone column and the surrounding soil within a column's zone of influence. Interface elements were introduced at the soil-column contact to allow for slippage. The interface strength was assumed to be 70% of the original soil strength (R_{int}= 0.7 in PLAXIS). Note that the interface properties have minimal effect on the results as the stone column is in triaxial state.

3.1 *Stone columns on rigid base*

Figure 3b presents the calculated n with depth for a particular case where embankment load is applied on stone columns that are founded on rigid base. The selected column configuration and parameters are shown in Figure 2. Note that the embankment fill was modeled as soil elements and the arching stresses developed above the column have been accounted for in the FEA model.

Clay: E′=3MPa, ϕ′=22°, c′=1kPa, γ_{total} = 17kN/m^3
Column: E′= 60MPa, ϕ′= 40°, c′= 0kPa, γ_{total} = 22kN/m^3
$\nu'_{clay} = \nu'_{column}$ = 0.3; b/a = 2; Ko = 0.5

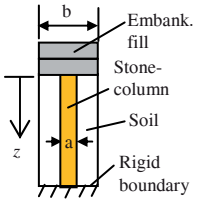

Figure 2. Stone column on rigid base

If the column and soil were appraised as elastic materials, the calculated n (dash line in Figure 3b) increases from 5 at the top of column, which is consistent with design chart solution provided in FHWA (1983) for embankment supporting columns, to about 14 at depth, which is commensurate with the equal strain solution (soil and column settle at the same rate at depth) given by Balaam and Poulos (1982).

When the column and soil are modeled as Mohr-Coulomb materials, yielding elements begin to form at the column top after a small load (~20kPa) is applied, leading to a reduction in stress concentration. The yielding of the column (hence the reduction of n) progresses downwards through the column as the applied load level increases (see the solid curves in Figure 3b). Figure 3a shows the stress state of the unit-cell model after the application of maximum embankment load. It indicates that most yielding elements are confined within the column periphery. The soil is generally elastic and therefore the soil friction angle has little influence on the solution.

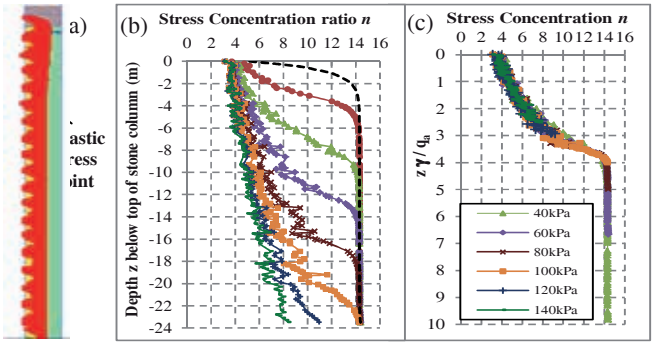

Figure 3. Stone column with rigid base (elasto-plastic solution)

Figure 3c shows a normalised plot in which the depth of the column, z, was normalised by q_a/γ, where q_a is the applied fill stress and γ is the total unit weight of the soil. It is found that the normalised stress concentration curves for the different load levels (≥ 40kPa) lie on a single curve. The turning point of the normalized curve corresponds to the transition from the upper yielding zone to the lower non-yielding zone, which occurs at different z for the different q_a. For example, point *A* in Figure 3c occurs at $z \cdot \gamma / q_a = 4$. When q_a=40kPa and γ=17kN/m^3, z = 9.5m (B in Fig 3b). Conversely, when q_a = 60kPa, z ≈ 14m (Point C).

Figure 4 presents a series of normalised curves for the n value under different modulus ratios, column spacing and friction angles of the stone column. For a given column spacing ratio and friction angle, the stress concentration is higher for higher modulus ratio E_c/E_s. Conversely, for the columns with a given modulus ratio, the extent of the yielding zone, and hence the reduction of stress concentration, is greater as the spacing ratio increases even though the maximum stress ratio in the columns is ultimately similar. This occurs because there is less confinement for the spaced columns, leading to greater yielding zone and stress reduction within columns. A comparison of the corresponding curves in Figures 4a and 4b shows that the loss of stress concentration due to yielding is more severe for column material having a lower angle of internal friction.

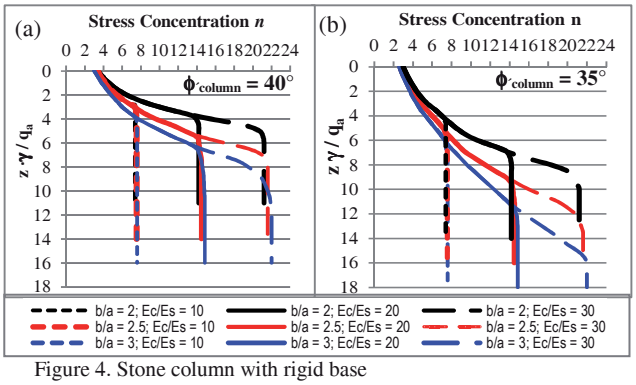

Figure 4. Stone column with rigid base

3.2 *Stone columns on compressible soils (elastic appraisal)*

For stone columns founded on compressible soil, the elastic FE solution has indicated that there exists a lower equal settlement plane, below which the columns move more than the soil to mobilise positive skin resistance of the soil. More load is transferred from the column to the surrounding soil and therefore the stress concentration n reduces (see Figure 5a).

Figure 5b shows a plot of normalised distance from the column base y/a (y and a defined in inset in Figure 5b) versus stress concentration reduction ratio r (= n / n_{max}) for the corresponding elastic FEA results given in Figure 5a. The n_{max} is the maximum computed n value based on elasticity as shown in Figure 5a. The FEA results for r near the column base can be approximated by the following logarithmic relationship.

$$r = 1 - \frac{1}{m}\left[log\left(\frac{\xi}{y/a}\right)\right] \quad \text{(for } y/a \le \xi\text{)} \qquad (3)$$

where ξ is the influenced zone (also normalized by the column diameter a) that is measured from the base of the column to the equal settlement plane (where r = 1). The magnitude of m controls the rate of reduction of r with y/d. The higher the m the more rapid reduction of r would be towards the column tip.

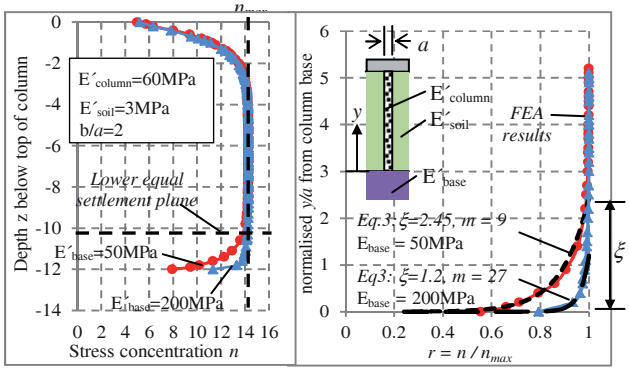

Figure 5. Stone column with compressible base -elastic solution

Figure 5b indicates that as the Young's modulus E_{base} of the soil beneath the columns increases, the extent of ξ reduces. Also, the ratio r reduces more rapidly towards the column tip (i.e. m increases) as E_{base} increases. Figure 6 presents the computed ξ and m for the different E_{base}/E_{column} and E_{base}/E_{soil} ratios based on elastic FEA. The following points can be drawn:

- The influenced zone ξ at the column base reduces as E_{base}/E_{column} increases. The reduction may be approximated by a straight line in ξ vs. log(E_{base}/E_{column}) plot. Curves 1 and 4 in Figure 6a delineate such relationships for column spacing b/a of 3 and 2, respectively. A curve in between representing b/a = 2.5 has not been shown for clarity of the figure. Note that these curves can apply to cases where $E_{base}/E_{soil} \ge 10$ as E_{soil} has negligible effect on the shape of r under this condition. For a particular b/a ratio, the ξ shows a

lower value as E_{base}/E_{soil} reduces to less than 10, although the trend of reduction with $\log(E_{base}/E_{column})$ remains linear and parallel with that for $E_{base}/E_{soil} \geq 10$ (curves 2 & 3, 5 & 6 in Figure 6a).

- The rate of reduction of r towards the column tip, represented by the m, has been found to increase linearly with E_{base}/E_{column}. Curve 7 in Figure 6b shows such relationship and is applicable for cases with different b/a ratio up to 3 (limit of parametric range) and with $E_{base}/E_{soil} \geq 10$. Curves 8 and 9 delineate the corresponding curves for cases with $E_{base}/E_{soil} = 2$ and 1.

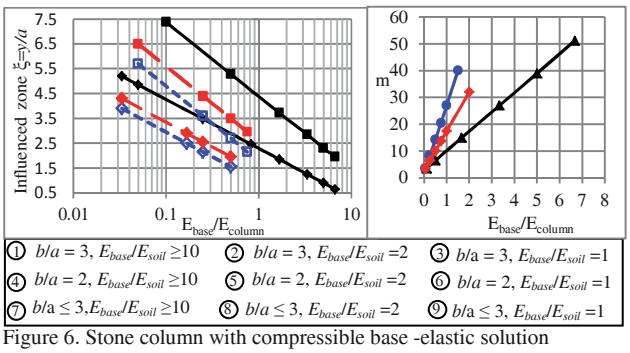

Figure 6. Stone column with compressible base -elastic solution

3.3 *Stone columns on compressible soils - elasto-plasticity*

The effect of compressible base on stress concentration n is now discussed based on Mohr Coulomb model. In particular, the soils surrounding and below the stone columns have been appraised alternatively using (i) effective shear strength (c, ϕ) and (ii) undrained shear strength s_u.

Figure 7a shows the computed n under different fill loads for the same case as in Figure 2,except that the column is founded on compressible soil that is represented by c-ϕ materials. The stress concentration curves initially follow identical paths as those shown in Figure 3b until they intercept the lower equal settlement plane and thereafter trace along the curve of the elastic solution at the column base. To explain this stress transfer mechanism, the material stress state of the model at the end of simulation (under 140kPa fill stress) is presented (inset in Figure 7a). As before, yielding of the column follows a top-down process. While there is significant yielding of the column due to high stress ratio, there is little yield in the surrounding soil especially towards the column base because of sufficient confinement even with an adopted soil friction angle as low as 22°. Since the soil is elastic, the reduction of n due to the compressible elastic base soil can be superimposed directly onto the aforementioned reduction due to yielding of column.

Figure 7b presents the results for the case where s_u = 30kPa has been adopted for the soils surrounding and below the column. Significant yielding occurs in the soils, which has altered the shape of the stress concentration curves towards the column base as compared to that of the c-ϕ soils. However the differences are not great and for the purpose of assessing n, the problem can be idealised by assuming that there is no failure in the surrounding soil so that its behavior is essentially elastic.

3.4 *Procedure for assessing stress concentration*

The following procedure for assessing the stress concentration of the stone columns under fill embankment may be proposed:

Step 1 – Assessing the stress concentration n along column depth by using charts such as Figure 4, which have accounted for the influence of load level, column spacing, modulus ratio of column and surrounding soil, and yield of the stone column.

Step 2 – Assess the influence of the compressible base soil on n based on elasticity by the following equation:

$$n = n_{max} \times r \qquad (4)$$

where r is the stress concentration reduction ratio given in Eq. 3, which is a function of ξ and m given in Figure 6. n_{max} is the maximum elastic n value below the turning point of each normalised $z \cdot \gamma / q_a$ – n curve in Figure 4.

Step 3 – Superimpose the solution from Step 2 onto that of Step 1. Thereby, the final n along the depth of the column is the lower of the two solutions at the same depth.

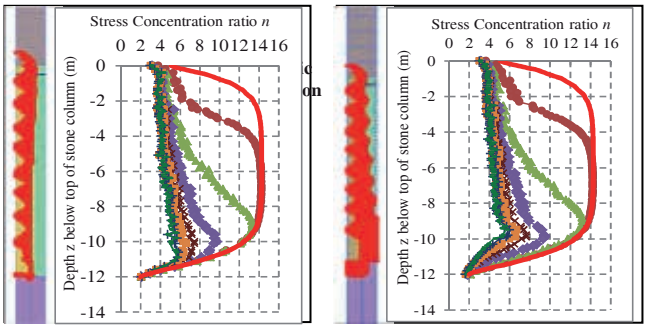

Figure 7. Stone column on compressible (a) c-ϕ and (b) s_u soil

4 COMPARISON WITH FULL 3-D MODELLING

The accuracy of plane strain idealisation of stone columns using equivalent strips in 2D FEA was investigated under self-weight load imparted by a 6m high embankment with 2H:1V batter. The analyses undertaken for the investigation include: *Analysis 1* - Full 3D FEA of embankment over stone columns modeled by solid elements; *Analysis 2* - Axisymmetric FEA of a unit cell consisting stone column; *Analysis 3* - 2D plane strain FEA with the stone columns modeled as strips; and *Analysis 4* - 2D FEA with the soil and columns modeled as equivalent block. The 2D and 3D FEA were carried out using software programme PLAXIS 2D and PLAXIS 3D, respectively.

Table 1 summarises the adopted parameters for all analyses. The 3D FEA is considered a baseline model that comprises a 13m long segment of embankment over soft clay treated with stone columns which are founded on compressible soil. The analysis was repeated with the 0.9m diameter stone columns spaced at 1.7m, 2m and 2.5m in triangular pattern. The 3D FE mesh is shown in Figure 8. The stone columns are modeled using 15 nodes wedge element with interface elements at the column-soil contact. Two cases of interface strength of 100% and 67% of the surrounding soil strengths have been considered.

Table 1. FEA Model Parameters

Analysis	***b/d***	***a_r***	***Stone Column Parameters***
1,2 3D FEA	2.0, 2.3, 2.9	0.26, 0.19, 0.12	E_{col}=50MPa, c_{col}=0kPa, ϕ_{col} = 40º
3 - 2D FEA (strips)	2.0	0.26	E_{strip}=26MPa, c_{strip}~1kPa, ϕ_{strip} = 36.5 - 38° along shaft , = 35.5 near base
	2.3	0.19	E_{strip}=22MPa, c_{strip}~1kPa, ϕ_{strip} = 35.5º-37° along shaft ; =34° near base
	2.9	0.12	E_{strip}=18MPa, c_{strip}~1kPa, ϕ_{strip} = 34.5º-35.5° along shaft; = 33° near base
4 - 2D FEA (equiv. block)	2.0	0.26	E_{block}=6MPa, c_{block}~1kPa,ϕ_{block} = 30º
	2.3	0.19	E_{block}=6MPa, c_{block}~1kPa, ϕ_{block} = 30º
	2.9	0.12	E_{block}=6MPa, c_{block}~1kPa, ϕ_{block} = 30º

Soil surrounding columns are E_{soil} = 3MPa, c_{soil} = 2kPa, ϕ_{soil} = 26º;
Soil beneath columns are E_{base} = 3MPa, c_{soil} = 5kPa, ϕ_{soil} = 28º

In Analysis 3, a 2D plane strain idealisation of the stone columns using equivalent strips was investigated. The strips are divided into several segments, each of which has different strength properties that correspond to the varying stress concentration along the column depth. The dimension and spacing of the 2D strips are as per those outlined in Figure 1.

Analysis 4 presents a conventional 2D approach in which the entire treated soil is represented by a single block with the

equivalent properties, ϕ_{block}, c_{block} and E_{block} derived based on the semi-empirical relationships given by Madhav, 1996.

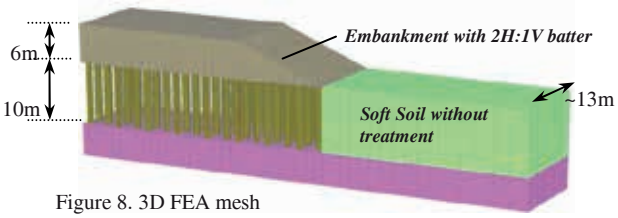

Figure 8. 3D FEA mesh

The baseline 3D model (Analysis 1) and the 2D strip model (Analysis 3) show similar deformation mechanisms of the stone columns, which can be broadly divided into three zones (see Fig 9a, 9b): Zone 1 away from the fill batter where columns underwent vertical deformation by "bulging"; Zone 2 just behind the crest of the fill batter where columns underwent both vertical and horizontal deformation by "bulging" and "leaning"; and Zone 3 beneath the fill batter where columns underwent mainly leaning. This numerical prediction of the deformation appears to be consistent with the results of the centrifuge model test carried out by Stewart and Fahey (1994). The maximum settlement of the embankment occurs in Zone 2 just before the crest of the fill batter (more than that in Zone 1). This is presumably due to the concurrence of bulging and leaning deformation mechanisms of the stone columns. Conversely, the columns in Zone 3 exhibit the maximum horizontal displacement and are likely due to the prevailing leaning deformation of the stone columns.

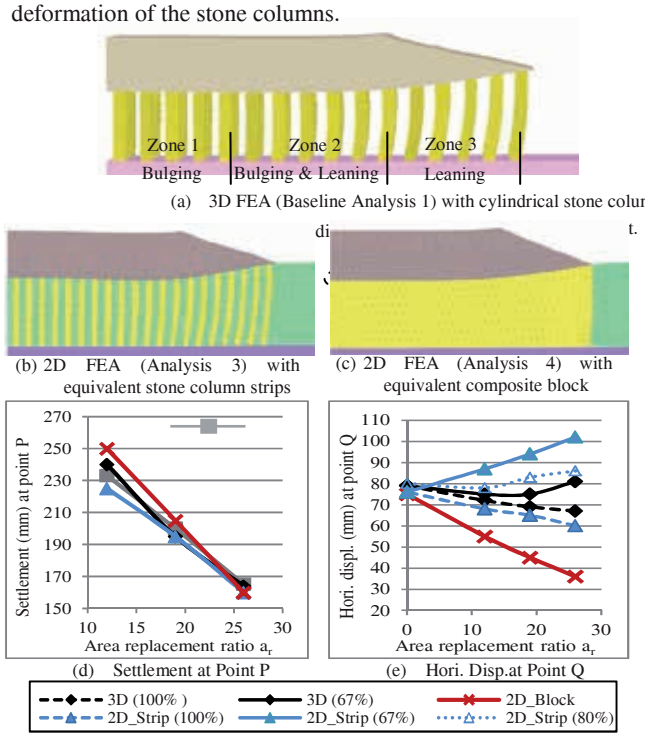

Figure 9. Comparison of FEA results

Figure 9c presents the deformation predicted by the conventional 2D FEA using composite block material (Analysis 4). This method is unable to capture the bulging and leaning deformation of the stone columns. The maximum settlement occurs at the centre of the embankment (i.e. in Zone 1) as opposed to in Zone 2 as predicted by the baseline 3D FEA and the proposed 2D FEA using equivalent strips.

Figure 9d shows a plot of predicted settlements at points P versus area replacement ratio a_r. All analyses give comparable results, indicating that all the different FE methods are commensurable in terms of settlement prediction under axially symmetric load condition.

Figure 9e presents the predicted horizontal displacement at point Q. The following points are drawn from the results:

- hen original soil strengths are used for the interface properties, the result of the 2D strip model (curve 1) compares well with that of the 3D baseline model (curve 2). Both results show a trend of reducing horizontal displacement with a_r.
- hen the interface strength of the columns in the 3D model are reduced to 67% of the soil strengths, the result (curve 3) indicates an initial drop off in horizontal displacement with a_r, but increases again once a_r > 20%. This is due to increasing proportion of yielding elements in the remolded soil as the columns draw closer to each other.
- he application of the same interface strength reduction (67% of surrounding soil strength) in the 2D equivalent strip model has caused excessive yield in the remolded soil and led to increased horizontal displacement with a_r (curve 4). A better fit to the 3D solution is by changing the interface strength to 80% of the surrounding soil strength (curve 5). Evidently, there needs a regime to determine an equivalent interface strength for the strip model. This merits further research.
- he 2D block model result (curve 6) under-predicts the horizontal displacement when compared with the 3D baseline model predictions. This indicates that the use of isotropic soil properties in the 2D block model, which were derived based on semi-empirical relationships originally for settlement prediction under axially loading condition, have overestimated the reduction in lateral spreading underneath the embankment batter. The use of equivalent strips in the 2D strip model is able to capture the interaction between the soil and the stone column, leading to a better agreement for the lateral deformation with the 3D baseline solution.

5 CONCLUSIONS

This paper presents a 2D FEA approach for analysing the response of stone columns under embankment loading. The stone columns are modeled as equivalent strips with the c_{eq} and E_{eq} of the strips calculated based on weighted average area approach, and the ϕ_{eq} derived based on force equilibrium method, which requires a presumption of stress concentration ratio of the stone column. For convenience, charts to assess the stress concentration ratio have been generated for full depth and floating stone columns. The solutions cover key parameters including load levels, column spacing ratio, E_{column}/E_{soil} ratio E_{base}/E_{column} ratio, E_{base}/E_{soil} ratio and column friction angles.

The accuracy of the proposed 2D strip model has been investigated by comparing the results of the 3D baseline FEA and the conventional composite approach. It has been shown that the proposed strip model is preferable over the conventional approach for the prediction of horizontal displacement. However, further research is needed to develop a regime to determine equivalent interface strength in the 2D strip method.

6 REFERENCES

Balaam, N.P. and Poulos, H.G. 1982. The behavior of foundations supported by clay stabilized by stone columns. *Proc. 8th European Conf. on Soil Mechanics and Foundation Engineering, Helsinki*.

FHWA. 1983. U.S. Department of Transportation Federal Highway Administration (Dec, 1983) – *Design and Construction of Stone Columns*, Vol 1. Report No. FHWA/RD-83/026.

Madhav,M.R. and Nagpure,D.D. 1996. Design of granular piles for embankments on soft ground. Proc. 12th SE Asian Geot.Conf., Kaula Lumpur. 1: 285-290

Stewart, D.P. and Fahey, M. (1994). Centrifuge modelling of a stone column foundation system, Seminar on ground improvement techniques , Perth, Curtin Printing Services, 1: pp 101-111.